EUROPEAN ORGANIZATION FOR NUCLEAR RESEARCH

L3 Note 2758
June 28, 2002

Measurement of the Scaling Property of the Factorial Moments in Hadronic Z Decay

The L3 Collaboration

Abstract

Both three- and one-dimensional studies of local multiplicity fluctuations in hadronic Z decay are performed using data of the L3 experiment at LEP. Normalized factorial moments in three dimensions are found to exhibit power-law scaling when partitioning with the same number of bins in each direction, indicating that the fluctuations are isotropic. This is confirmed by a detailed study of the second-order factorial moments in one dimension. Such scaling corresponds to a self-similar fractal, *i.e.*, the associated branching process is self-similar. On the contrary, two-jet subsamples are found to have self-affine branching. These features are at least qualitatively reproduced by the Monte Carlo models JETSET 7.4 and HERWIG 5.9. *These results are preliminary.*

Submitted to the 31^{st} *International Conference on High Energy Physics*
Amsterdam, Netherlands, 24-31 July 2002.

1 Introduction

QCD branching [1], like other branching processes [2], leads to fractal behavior [3]. This fractal behavior manifests itself in the form of power-law scaling of final-state multiplicity fluctuations with increasing resolution in phase space [4,5]. Experimentally, approximate power-law scaling is indeed observed, not only in e^+e^- collisions, but, be it of reduced strength, also in all other types of collisions [6]. To be able to distinguish QCD branching expected to be present in e^+e^- collisions from the dynamics at work in hadron-hadron collisions, a more precise discriminator is needed.

When the underlying space is of dimension two or higher, there are two distinct kinds of fractals, self-similar and self-affine [2]. The difference between these two lies in the scales used in the different space directions. If the power-law scaling holds when the underlying space is partitioned equally in all directions (see Fig. 1a) , the corresponding fractal is called *self-similar*. If, on the other hand, power-law scaling holds when and only when the partitioning is different in different directions (Fig. 1b and c), the corresponding fractal is called *self-affine*. An example of the latter is the three-dimensional landscape, where the vertical direction is distinguished from the horizontal ones by gravity. Translated into the language of multiplicity fluctuations in phase space, self-similar behavior corresponds to isotropic multiplicity fluctuations, while self-affine behavior corresponds to non-isotropic fluctuations.

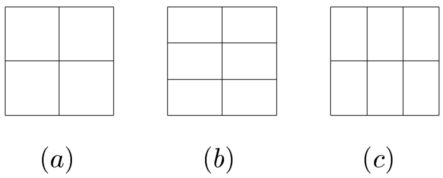

Figure 1: Schematic sketch of isotropic (a) and anisotropic (b and c) partitioning of phase space in two dimensions.

It has been observed [7], using Z-decay data [8] and JETSET [9], that QCD branching may correspond to a *self-similar* fractal. This was qualitatively confirmed in Ref. 10 and can be understood from the fact that transverse momenta are not limited to small values in the early hard stages of the branching process. If true, this has to be contrasted with the anisotropic fluctuations corresponding to a *self-affine* behavior observed in hadron-hadron collisions at lower center-of-mass energies (22–27 GeV) [11–13].

Expressed in terms of normalized factorial moments (NFM) [4,5], which are generally used as a tool to study multiplicity fluctuations [6], the 3-dimensional NFM of hadrons produced in e^+e^- collisions are expected to exhibit a power-law scaling property when phase space is partitioned isotropically, while the scaling in hadron-hadron collisions only occurs when phase space is partitioned anisotropically.

In this paper, we quantitatively study the exact scaling property of the NFM in the hadronic final state of e^+e^- collisions, using the hadronic Z decay data obtained in the L3 detector [14] at LEP. Besides in the full data sample, we will also analyze the scaling property of the NFM in the two-jet sub-sample and its dependence on the jet resolution parameter y_{cut}, which can help in understanding the transition between perturbative and non-perturbative processes.

2 Method of analysis

In cosmic-ray [15] and accelerator [16] experiments, local multiplicity fluctuations have been found to be 2 to 60 times the average particle density. These observations suggest that the local multiplicity fluctuations may not be purely statistical, but may have non-statistical, *i.e.*, dynamical origin.

Dynamical fluctuations can be studied using the normalized probability moments,

$$C_q(M) = \frac{1}{M} \sum_{m=1}^{M} \frac{\langle p_m^q \rangle}{\langle p_m \rangle^q} \ , \tag{1}$$

where a region Δ in 1-, 2- or 3-dimensional phase space is partitioned into M cells and p_m is the probability of finding a particle in the cell m. Further, $\langle \cdots \rangle$ denotes an average over the event sample,

$$\langle \cdots \rangle = \frac{1}{N_{\rm ev}} \sum_{i=1}^{N_{\rm ev}} (\cdots)_i \ , \tag{2}$$

where $N_{\rm ev}$ is the number of events in the sample. If the underlying dynamical fluctuations are intermittent rather than continuous, the C_q will exhibit power-law scaling [4, 5]:

$$C_q(M) \propto (M)^{\phi_q} \qquad (M \to \infty) \ . \tag{3}$$

Normalized factorial moments (NFM) are defined by

$$F_q(M) = \frac{1}{M} \sum_{m=1}^{M} \frac{\langle n_m(n_m-1)\cdots(n_m-q+1) \rangle}{\langle n_m \rangle^q} \ , \tag{4}$$

where n_m is the multiplicity in cell m. The $F_q(M)$ are equal to the probability moments $C_q(M)$ provided that the statistical fluctuations are Poissonian [5]. Thus the dynamical fluctuations can be explored by studying the power-law scaling of the NFM

$$F_q(M) \propto (M)^{\phi_q} \qquad (M \to \infty) \ . \tag{5}$$

If this power-law scaling (intermittency) is observed then the corresponding hadronic system is fractal [2].

In higher dimensions, the observation or non-observation of power-law scaling, Equation (5), of the NFM depends on how phase-space is partitioned. For example, if in the two-dimensional case (a, b plane) the power-law scaling of the NFM is observed when phase space is divided equally in different directions, *i.e.*, when the partition numbers M_a and M_b in directions a and b are equal, as is illustrated in Fig. 1a, then the dynamical fluctuations are isotropic and the corresponding fractal is *self-similar*. On the other hand, if the power-law scaling of the NFM is observed when and only when phase space is divided differently in different directions, *i.e.*, when $M_a \neq M_b$, as in Fig. 1b or c, then the dynamical fluctuations are anisotropic and the corresponding fractal is *self-affine* [11–13, 17]. The degree of anisotropy can be characterised by the log-ratio of M_a and M_b *)

$$H_{ab} = \frac{\ln M_a}{\ln M_b} \ , \tag{6}$$

*) In observing the power law scaling property of a system, the phase space region in direction i is partitioned into λ_i bins, and then each bin is further partitioned into λ_i sub-bins, ... After ν steps, the partition number in direction i is $M_i = \lambda_i^\nu$. In this process, it is the log-ratio of M_a and M_b rather than their ratio itself that remains constant and can be used as a characteristic quantity.

which is called the Hurst exponent [2]. The dynamical fluctuations are isotropic in the (a, b) plane if $H = 1$ and anisotropic in this plane if $H \neq 1$ [17]. The farther the Hurst exponent departs from unity, the stronger the degree of anisotropy.

A second point to be noted is that the multiparticle final state of a high energy collision is a three-dimensional object. So, power-law scaling of the NFM is expected to manifest itself in three-dimensional phase space. Consequently, when evaluated in one dimension, the NFM will saturate due to projection [18]. The second-order NFM can be written

$$F_2^{(a)}(M_a) = A_a - B_a M_a^{-\gamma_a} \ , \tag{7}$$

and the Hurst exponent in the (a, b) plane is related to the exponents γ_a and γ_b through [19]

$$H_{ab} = \frac{\ln M_a}{\ln M_b} = \frac{1+\gamma_b}{1+\gamma_a} \ . \tag{8}$$

Consequently, the condition $H_{ab} = 1$, which implies isotropic dynamical fluctuations in the (a, b) plane, is equivalent to the condition $\gamma_a = \gamma_b$.

The primary product of Z decay considered here is a quark-antiquark pair, moving back to back in the Z rest frame. This implies a cylindrical symmetry about the quark direction. An appropriate frame to study the development of the $\mathrm{q\overline{q}}$ system is therefore defined by this direction, and appropriate variables are the longitudinally Lorentz invariant variables rapidity y, transverse momentum p_t and azimuthal angle φ. The $\mathrm{q\overline{q}}$ direction is approximated by the thrust axis, defined as the direction $\vec{n}$ which maximizes the expression [20]

$$T = \frac{\sum_i \vec{n} \cdot \vec{p}_i}{\sum_i |\vec{p}_i|} \ , \tag{9}$$

where the sum runs over all particles of the event. Maximizing a similar expression in the plane perpendicular to the thrust axis, yields the 'major' axis [21]. The direction perpendicular to both of these two axes gives the 'minor' axis. Using these three axes as a basis, a Cartesian coordinate system can be constructed. By convention, we define the z axis of this frame parallel to the thrust axis and the y axis parallel to the major axis. We refer to this frame as the thrust frame.

Crudely speaking, for a multi-jet event the thrust axis is the direction of the primary quark and anti-quark originating from the decay of the Z, while the major axis is determined by the direction of the first hard gluon emission. Using the major and minor axes as the coordinates in the plane perpendicular to the thrust axis means that the azimuthal angle of the direction of the first hard gluon emission is fixed to $\pi/2$. Thus, fluctuations in this angle, if any, will be largely reduced [7]. We have used two methods to relax this limitation in order to observe the fluctuations fully. The first method [7] is to rotate the coordinate system around the thrust axis and to define a new x axis as lying in the z_0-z plane, where z_0 points along the $\mathrm{e^+e^-}$ beam direction. The second method is to simply choose a random number distributed uniformly in the interval $[0, 2\pi]$ and to add this to the azimuthal angle of every particle in the event. This is equivalent to a rotation of the coordinate system around the thrust axis by a random angle. Experimentally, one can expect the second method to be somewhat superior, since it is defined independent of the detector and thus avoids some possible systematic effects. In practice, we have found the results of the two methods completely compatible. Consequently we refrain from presenting the results based on the beam direction.

The power-law scaling property of the NFM is studied in the thrust frame and in the randomly rotated frame, which we refer to as the random frame. Since the thrust axis is only an approximation of the $q\overline{q}$ axis, we also present the NFM's after a Monte Carlo correction for this. We refer to this frame as the $q\overline{q}$ frame.

The analysis uses nearly the entire phase space: $[-5 \leq y \leq 5]$, $[-\pi \leq \varphi < \pi]$, $[0.1 \leq p_{\mathrm{t}} \leq 3$ GeV$]$. In order to avoid the influence of the non-uniformity of the distributions of these variables, all variables are transformed into their corresponding cumulative forms [22]. For 1-D distributions this results in partitioning such that the mean number of entries in each bin is the same. For 3-D distributions, the approximation is often used that the three variables y, p_{t} and φ are independent, in which case the same partitioning can be used as found in the three 1-D cases. However, the three variables are not independent—particularly for large values of $|y|$, in which case large values of p_{t} are suppressed. Consequently we use a more elaborate method of partitioning [23] whereby first one variable is partitioned as in the 1-D case. Then, for each bin of the first variable, the second variable is partitioned. Finally, the third variable is partitioned for each 2-D bin of the first two variables. This results in bins which all have the same average occupancy. Although, the prescription is not unique in that it depends on the order in which the three variables are treated, the differences in the F_q obtained are found to be neglibible compared to the statistical errors.

In order to eliminate the influence of momentum conservation [24], the first point (corresponding to $M = 1$) is not used in fits of the the 3-D F_q *vs.* M data, and the first 1–3 points are not used in fits of Equation (7) to the 1-D F_2 *vs.* M data.

We first investigate the 3-D NFM, partitioning phase space isotropically. Observation of a linear dependence of $\ln F_q$ on $\ln M$ is then a direct indication of the isotropy of the dynamical fluctuations. More quantitative evidence is found by fitting Equation (7) to the three 1-D F_2's. Isotropy of the dynamical fluctuations will manifest itself in an equality of the three γ's, or equivalently in a unit value of the three Hurst exponents calculated from the γ's via Equation (8).

Since the particle production mechanism in hadronic Z decay consists of two parts, a perturbative parton branching and a non-perturbative fragmentation, it is unclear whether the results (isotropy or anisotropy of the dynamical fluctuations) obtained from the full data sample is due to the perturbative or the non-perturbative process.

In order to study this point, we construct a sub-sample of 2-jet events using the Durham algorithm [25, 26]. The definition of "2-jet sample" depends on the jet resolution parameter y_{cut} used in the algorithm. When y_{cut} is very small, the production mechanism in the 2-jet sample is mainly non-perturbative hadronization. When y_{cut} is very large, the "2-jet sample" coincides with the full event sample and the full perturbative parton branching enters into these "jets", together with the non-perturbative hadronization. Thus, a study of the variation of the scaling property with y_{cut} explores the role of perturbative and non-perturbative processes in the isotropy or anisotropy of the dynamical fluctuations.

3 Data sample

The data used in the analysis were collected by the L3 detector [14] in 1994 at a center-of-mass energy $\sqrt{s} \simeq 91.2$ GeV. Events are selected in a two-step procedure [27, 28]. First, at least 15 calorimetric clusters of at least 100 MeV are required in order to reduce background from the $e^+e^- \to \tau^+\tau^-$ process. Hadronic events are then selected by requiring small energy imbalance both along and transverse to the beam direction:

$$0.5 < \frac{E^{\rm cal}}{\sqrt{s}} < 1.5, \quad \frac{|E_{\parallel}^{\rm cal}|}{E^{\rm cal}} < 0.4 \quad \text{and} \quad \frac{|E_{\perp}^{\rm cal}|}{E^{\rm cal}} < 0.6 \ ,$$

where $E^{\rm cal}$ is the total calorimeter energy, $E_{\parallel}^{\rm cal}$ is the energy imbalance along the beam direction, and $E_{\perp}^{\rm cal}$ is the energy imbalance perpendicular to the beam direction. To ensure that the event fully lies within the acceptance of the calorimeter, selected events are required to have $|\cos\theta_{\rm th}^{\rm cal}| \leq 0.74$, where $\theta_{\rm th}^{\rm cal}$ is the polar angle of the event thrust axis determined from calorimeter clusters.

The second step is the selection of charged tracks measured in the central tracker and the silicon micro-vertex detector. A number of quality cuts are used to select well-measured tracks. Further, the thrust direction calculated from the charged tracks is required to lie within the full acceptance of the central tracker: $|\cos\theta_{\rm thr}| < 0.7$, where $\theta_{\rm thr}$ is the polar angle of the thrust axis determined from charged tracks only. The track selection efficiency, determined from Monte Carlo, is about 75%. A small remaining background of $\tau^+\tau^-$ events in which both τ particles decay into more than one charged particle is removed by requiring the second largest angle φ_2 between any two neighboring tracks in the $R-\varphi$ plane to be less than $170°$. After this cut the $\tau^+\tau^-$ contamination is approximately $8\cdot 10^{-5}$. The resulting data sample consists of approximately 0.8 million hadronic events, and has a purity greater than 99%.

To determine the thrust axis, and to classify events as having two jets, we use a combination of calorimeter clusters and charged tracks.

In this paper we study fluctuations in small angular bins. For the grouping of tracks into these bins, the resolution of the angle between pairs of tracks is of crucial importance. For this reason we impose an additional cut, requiring an unambiguous polar angle measurement. Together with the previous cuts about 40% of the tracks are rejected. With this selection we achieve good agreement between data and simulation for the distributions of the difference in angle between pairs of tracks for both the azimuthal angle about, and the polar angle with respect to the beam, as is shown in Fig. 2.

The resolution of the L3 detector for the difference in y, $p_{\rm t}$, and φ between two tracks is estimated to be 0.05, 0.03 GeV, and 0.03 radians, respectively [28]. The widths of the smallest bins used ($M = 40$) are roughly 3–5 times these values.

An NFM calculated from the data is corrected for detector effects by a correction factor determined from the following two Monte Carlo (MC) samples.

1. A generator level MC sample generated directly from the JETSET 7.4 parton shower program [9]. This contains all charged final-state particles with a lifetime $c\tau > 1$ cm and is generated without initial-state photon radiation (ISR), while Bose-Einstein (BE) correlations are included using the so-called BE_0 algorithm [29].
2. Events generated with JETSET 7.4 including ISR and BE correlations are passed through a full detector simulation [30] including time-dependent variations of the detector response based on continuous detector monitoring and calibration. The sample is reconstructed with the same program as the data and passed through the same selection procedure. It is referred to as detector level MC. As seen in Figure 2, this MC provides a reasonable description of the data.

From these two MC samples a correction factor is found: $R_q = F_q^{\rm gen}/F_q^{\rm det}$, where $F_q^{\rm gen}$ and $F_q^{\rm det}$ are the values of the NFM of order q calculated from the generator-level and detector-level

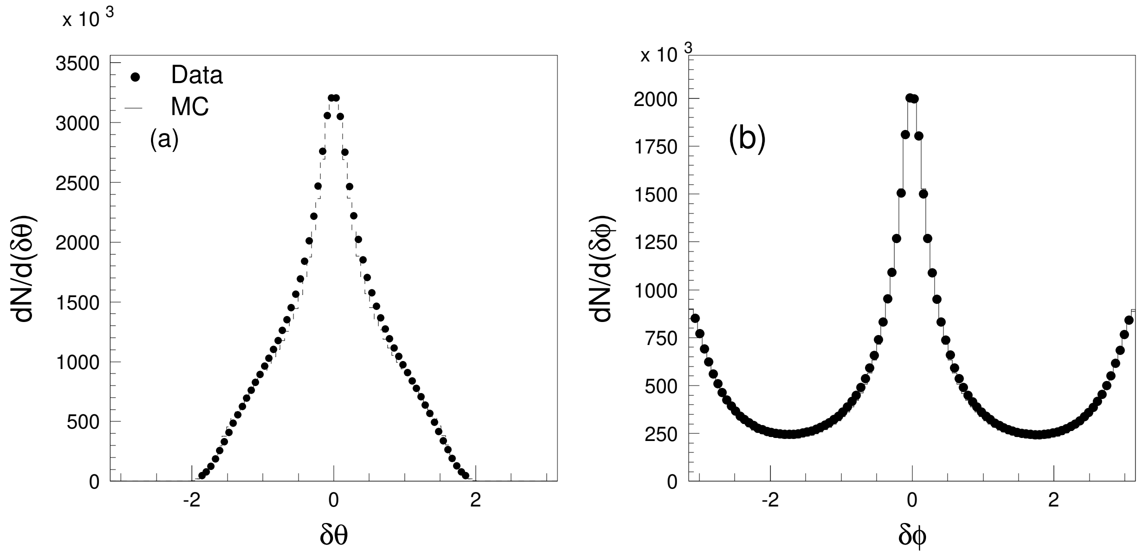

Figure 2: The distribution of the difference in angle between pairs of selected tracks for the polar angle (a) and azimuthal angle (b).

MC, respectively. The corrected NFM is then given by $F_q = R_q\, F_q^{\rm raw}$, where $F_q^{\rm raw}$ is the NFM calculated directly from the data. These corrections, which increase with M and with q, are about 1–8%.

4 Systematic uncertainties

Systematic uncertainties on the factorial moments have been assigned [28] for the following sources: event selection, track selection, Monte Carlo modeling for the detector correction. For the selections, the cuts used were varied between reasonable limits. For each cut, the maximum difference between the value found using the standard cut and varied cuts was taken as the uncertainty from that cut. Similarly, the uncertainty from MC modeling was determined by using JETSET without BE correlations and HERWIG, instead of JETSET. These uncertainties were added in quadrature to obtain the total uncertainty. For the $q\overline{q}$ frame there is an additional contribution from MC modeling of the correction from thrust axis to $q\overline{q}$ direction. This is taken from the variation in the correction factor found using the three Monte Carlos.

For the comparison of experimental data to MC models, the systematic errors of the models are calculated by changing their parameters by one standard deviation from their L3-tuned values [31]. Systematic errors on fit results are determined by repeating the analysis using charged tracks, rather than calorimeter clusters, for event selection and to determine the thrust axis.

5 Results for the full data sample

The results for the 3-D NFM's, using the same number of bins in each direction, are shown in Fig. 3 for the thrust, random, and $q\overline{q}$ frames. The error bars include both statistical and systematic uncertainties. They are highly correlated for neighboring values of M. Disregarding the first point, which is heavily influenced by momentum conservation, the $\ln F_q^{\rm 3D}$ appear

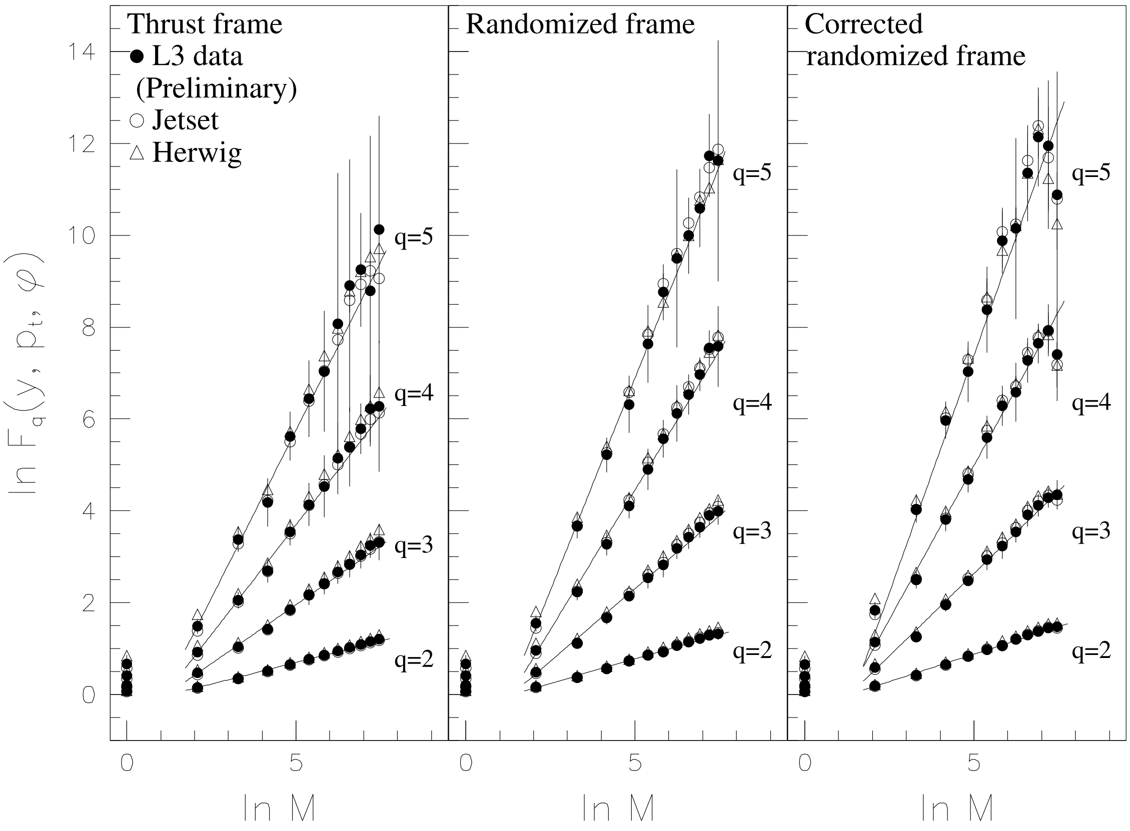

Figure 3: The three-dimensional factorial moments as a function of the number of partitions $M = M_y M_{p_t} M_\varphi$, $M_y = M_{p_t} = M_\varphi$, compared to JETSET with BE and to HERWIG in the (a) thrust, (b) random, and (c) $\mathrm{q\overline{q}}$ frames, respectively. The error bars include both statistical and systematic uncertainties.

to depend linearly on $\ln M$ for this isotropic partitioning, as is expected if the dynamical fluctuations in hadronic Z decay are isotropic. This appears true for the thrust frame as well as for the random and $\mathrm{q\overline{q}}$ frames, although the slopes are smaller in the thrust frame. The NFM's for JETSET and HERWIG are also shown in the figure. Both agree well with the data.

In order to investigate the isotropy of the fluctuations more quantitatively, we study the one-dimensional NFM for the three variables y, p_t and φ, separately. They are plotted in Figure 4 for the thrust and random frames, and compared to JETSET and HERWIG. Since these frames have the same z-axis, only $F_2(\varphi)$ depends on which frame is used. It is clear from the figure that the fluctuations in φ are strikingly different in the two frames, being nearly absent in the thrust frame. This difference is attributed to the limitation, in the thrust frame, of the direction of the first hard gluon emission to the (y, z) plane as discussed in Section 2. As a consequence of the reduced fluctuations in φ, the fluctuations in three dimensions are also reduced, resulting in the lower values of the NFM's in the thrust frame observed in Fig. 3a. Figure 5 shows the comparison for the $\mathrm{q\overline{q}}$ frame. In all frames, the data are well-described by JETSET, both with and without BE, and somewhat less well by HERWIG.

Equation (7) is fit to the data of Figures 4 and 5 using the full covariance matrix for the statistical and systematic errors. The results are shown in Table 1. We find, both for the random frame and the $\mathrm{q\overline{q}}$ frame, that the values of γ_y, γ_{p_t} and γ_φ are equal as expected for isotropic fluctuations, although the values are shifted somewhat lower in the $\mathrm{q\overline{q}}$ frame.

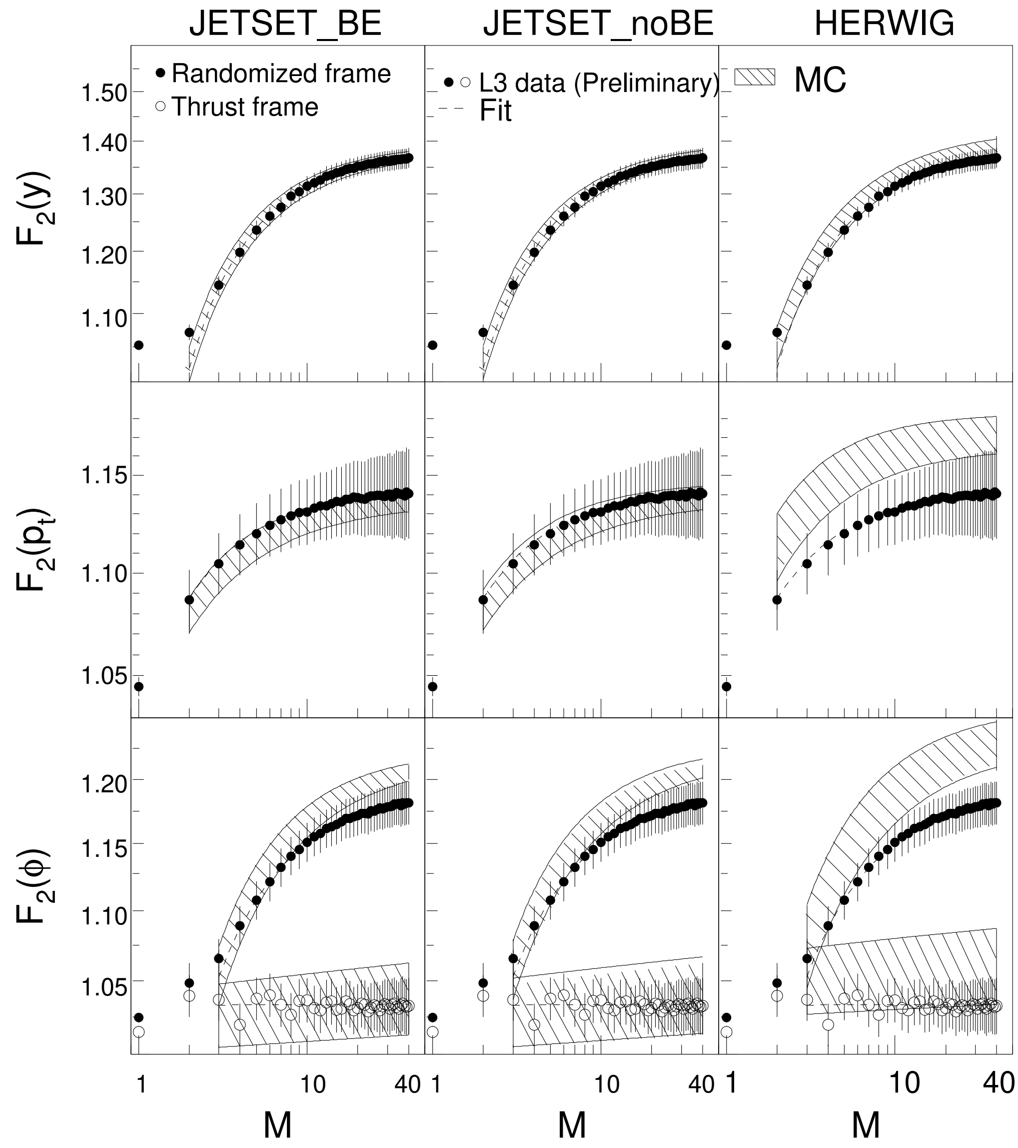

Figure 4: The 1-D second-order factorial moments as a function of partition number M in the random frame (squares) and in the original thrust frame (open circles) compared to (a) JETSET with Bose-Einstein, (b) JETSET without Bose-Einstein, and (c) HERWIG. The error bars on the data are the combined statistical and systematic uncertainties. The hatched bands indicate the systematic uncertainty of the MC models. The dashed lines indicate the results of the fits of Equation 7.

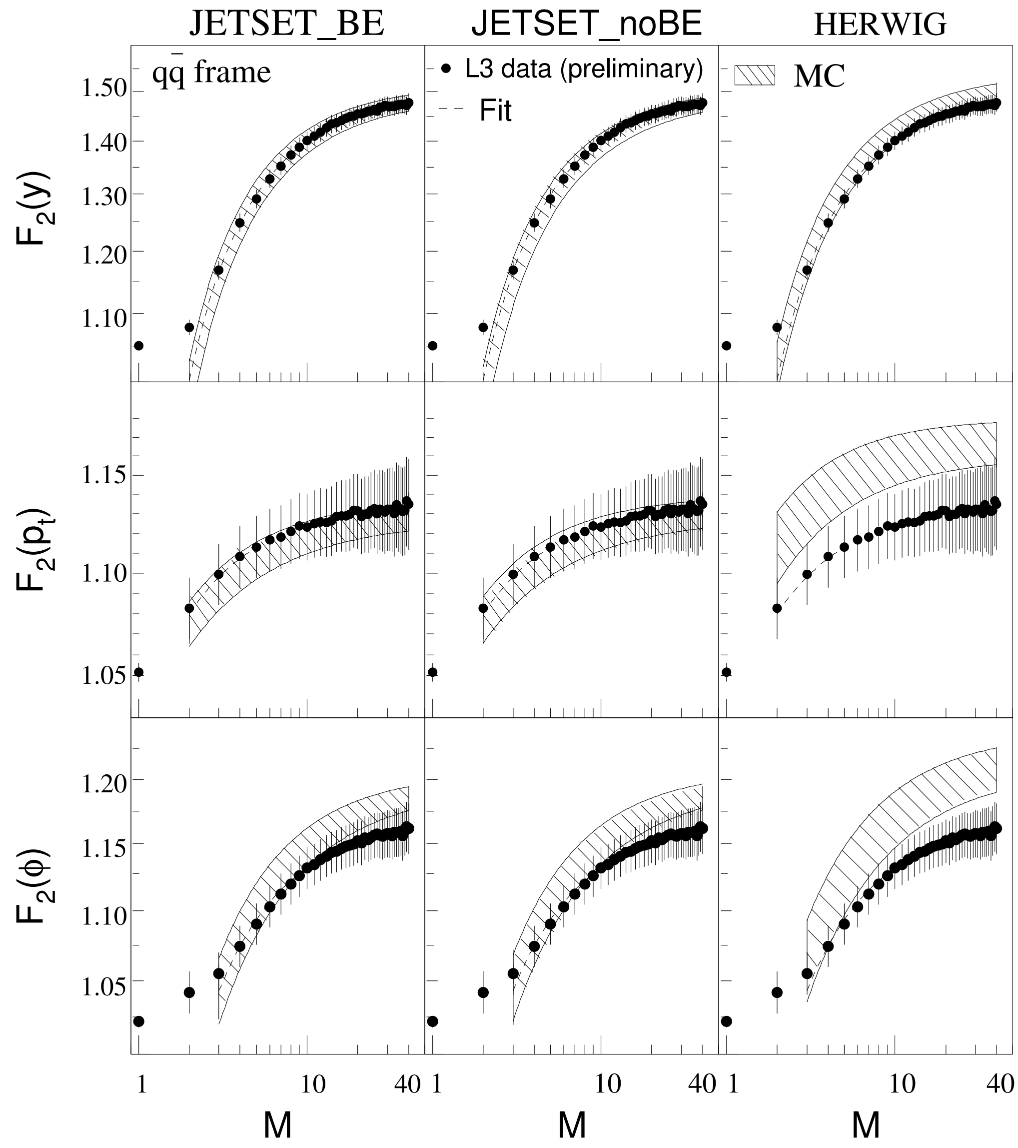

Figure 5: The 1-D second-order factorial moments as a function of partition number M in the q$\overline{\text{q}}$ frame compared to (a) JETSET with Bose-Einstein, (b) JETSET without Bose-Einstein, and (c) HERWIG. The error bars on the data are the combined statistical and systematic uncertainties. The hatched bands indicate the systematic uncertainty of the MC models. The dashed lines indicate the results of the fits of Equation 7.

Frame	Variable	γ	χ^2/dof
Random	y	$0.992 \pm 0.014 \pm 0.028$	36/36
	p_t	$0.986 \pm 0.022 \pm 0.032$	29/37
	φ	$0.993 \pm 0.024 \pm 0.033$	25/35
$q\overline{q}$	y	$0.966 \pm 0.019 \pm 0.018$	35/36
	p_t	$0.972 \pm 0.042 \pm 0.030$	31/37
	φ	$0.967 \pm 0.034 \pm 0.024$	27/37

Table 1: The fit parameters, γ_i, of fits of Equation (7) to the 1-D NFM for the data. The first error is the combined statistical and systematic uncertainties from event and track selection and MC modeling; the second combines the systematic uncertainties arising from choice of event selection method and of thrust axis determination.

H_{yp_t}	0.997±0.018±0.030	Data - Random frame
	1.003±0.031±0.024	Data - $q\overline{q}$ frame
	0.978±0.016±0.042	JETSET
	1.079±0.026±0.058	HERWIG
$H_{y\varphi}$	1.001±0.019±0.031	Data - Random frame
	1.001±0.027±0.021	Data - $q\overline{q}$ frame
	0.991±0.014±0.033	JETSET
	1.015±0.025±0.033	HERWIG
$H_{p_t\varphi}$	1.003±0.023±0.033	Data - Random frame
	0.996±0.038±0.027	Data - $q\overline{q}$ frame
	1.014±0.017±0.055	JETSET
	0.940±0.022±0.047	HERWIG

Table 2: Hurst exponents for the random and $q\overline{q}$ frames compared to JETSET with BE and HERWIG. The uncertainties are as in Table 1.

From these values of γ, the Hurst exponents are calculated by Equation (8). The resulting values are displayed in Table 2, where they are compared to the values obtained for JETSET and HERWIG. They are, for both data and MC's, consistent with unity, in agreement with isotropic dynamical fluctuations.

Since the dynamical fluctuations appear to be isotropic in the random and $q\overline{q}$ frames, the 3-D F_q can be fit by

$$F_q^{3\mathrm{D}} = b_q M_{3\mathrm{D}}^{\phi_q} \ , \qquad (10)$$

to obtain physically meaningful intermittency indices ϕ_q. The results of the fits, using the full covariance matrix, are shown in Table 3 and displayed in Figure 3. The first error includes both the statistical error and the systematic uncertainties from event and track selection as well as from Monte Carlo modeling. The second is the systematic uncertainty from the method of event selection and from the definition of the thrust axis. For comparison, we also show the results of fits in the thrust frame in order to illustrate the dependence on the correct choice of frame. In the thrust frame the ϕ_q are much lower than in the other frames, as a consequence of the dependence of this frame on the QCD dynamics, as discussed above. We also note that the ϕ_q are systematically higher in the $q\overline{q}$ frame than in the random frame, from which we

Frame	order, q	ϕ_q	χ^2/dof
Thrust	2	$0.187 \pm 0.004 \pm 0.015$	7.4/9
	3	$0.512 \pm 0.012 \pm 0.029$	7.7/9
	4	$0.954 \pm 0.030 \pm 0.049$	5.8/9
	5	$1.463 \pm 0.051 \pm 0.003$	6.6/9
Random	2	$0.212 \pm 0.005 \pm 0.004$	10.3/9
	3	$0.632 \pm 0.016 \pm 0.014$	9.9/9
	4	$1.215 \pm 0.028 \pm 0.016$	9.6/9
	5	$1.847 \pm 0.042 \pm 0.036$	7.0/9
$\mathrm{q\overline{q}}$	2	$0.239 \pm 0.007 \pm 0.005$	5.9/9
	3	$0.717 \pm 0.016 \pm 0.025$	8.4/9
	4	$1.340 \pm 0.028 \pm 0.059$	7.8/9
	5	$2.167 \pm 0.052 \pm 0.210$	9.8/9

Table 3: Intermittency indices, ϕ_q, from fits of Equation (10) to the three-dimensional factorial moments in different frames. The uncertainties are as in Table 1.

conclude that the difference between the thrust and $\mathrm{q\overline{q}}$ axes, which also depends on the QCD dynamics, also serves to decrease the observed fluctuations.

6 Results from the "2-jet" sub-sample

Now we turn to the study of the "2-jet" sub-sample. The "jets" are identified using the Durham jet algorithm [25,26]. The jet resolution parameter y_{cut} used in this algorithm is essentially the relative transverse momentum squared [32],

$$k_{\mathrm{t}}^2 = y_{\mathrm{cut}} \cdot s \ , \tag{11}$$

where the center-of-mass energy, $\sqrt{s}$, is equal to 91.2 GeV in our case.

The fraction R_2 of "2-jet events" obtained through the jet-algorithm depends on the parameter y_{cut}. The dependence, as found using JETSET, is shown in Fig. 6, together with the fractions R_3, R_4 and $R_{5\mathrm{m}}$ of 3-jet, 4-jet and 5-or-more-jet events, respectively.

It is worthwhile noting that R_2 tends to zero at around $k_{\mathrm{t}} = 1$ GeV. This can be understood in the following way [33]. Consider an event with only two hard partons having no perturbative branching at all. This is certainly a 2-jet event. However, even in this case the two partons still undergo non-perturbative hadronization to produce final-state particles. If we choose $k_{\mathrm{t}} < 1$ GeV, then the non-perturbative hadronization will be considered to produce new "jets" and this 2-jet event will be taken as a "multi-jet" event.

When k_{t} increases, the ratio R_2 of 2-jet events increases, and more and more parton branchings are included in the jets. In the extreme case, when y_{cut} is very large, the "2-jet sample" coincides with the full sample and contains all the information on hard parton branching as well as on soft hadronization.

The NFM is calculated from the 2-jet sample for different y_{cut} values. The random frame is used throughout. The variation with R_2 of the exponents γ_i ($i = y, p_{\mathrm{t}}, \varphi$) are plotted in Fig. 7 for data and for JETSET with BE_0 and HERWIG.

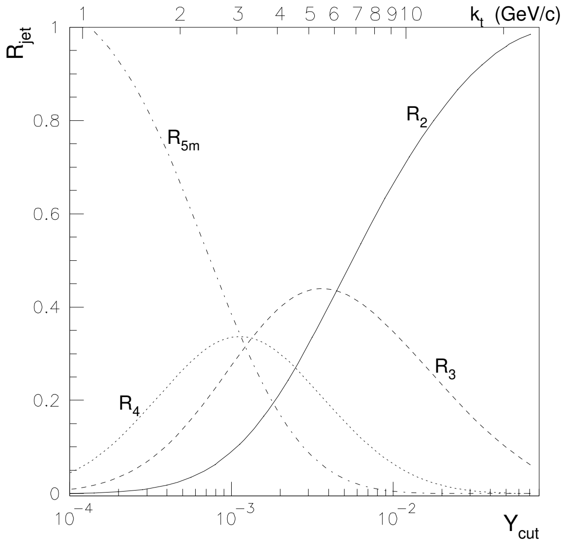

Figure 6: The dependence of 2-, 3-, 4-, 5-or-more-jet event fractions on the jet resolution parameter $y_{\rm cut}$, as found using JETSET.

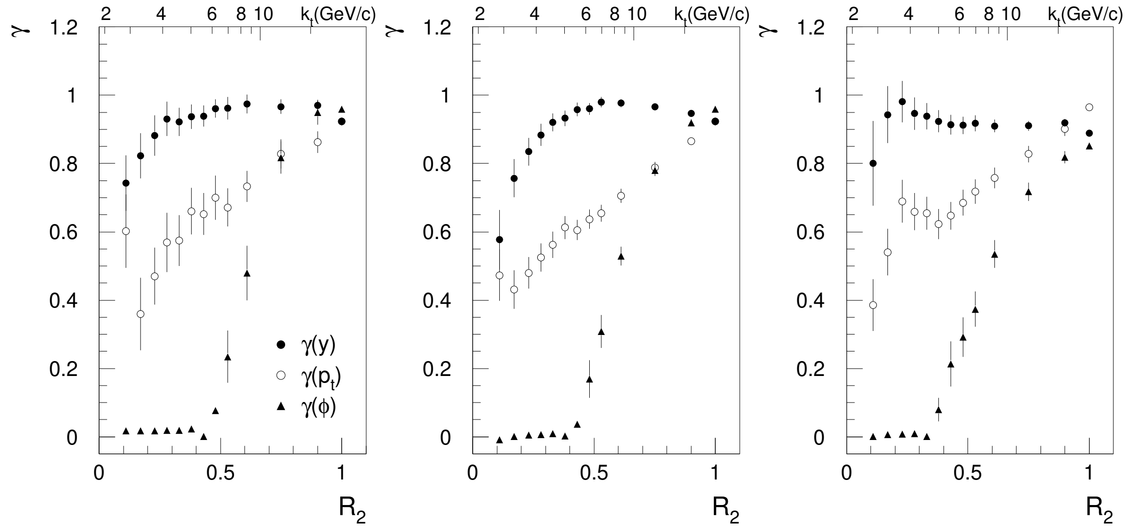

Figure 7: The variation of γ_i $(i = y, p_{\rm t}, \varphi)$ with R_2 and $k_{\rm t}$ for (a) data, (b) JETSET and (c) HERWIG.

At low R_2 and k_t, where almost all genuine two-jet events are split up and only the 'skinniest' survive, all three exponents γ are small, indicating only marginal dynamical fluctuations. On the contrary, at R_2 near 1, all three exponents are large and equal, in agreement with the strong and isotropic fluctuations in the full sample discussed in the previous section. While γ increases with k_t (or $y_{\rm cut}$) for each of the variables, the dependence on $y_{\rm cut}$ is very different for the different variables, y, p_t and φ. Somewhat similar behavior is seen for JETSET and HERWIG.

7 Conclusions

The scaling property of the three-dimensional factorial moments of the hadronic system produced in Z decay is examined using the high statistics data from the L3 experiment at LEP. The results show power-law scaling when phase space is partitioned isotropically in a coordinate frame which does not depend on the QCD dynamics, indicating the existence of self-similar (isotropic) dynamical fluctuations. This self-similarity is confirmed quantitatively by fits to the one-dimensional F_2. This is in sharp contrast to the self-affine (anisotropic) fluctuations observed in hadron-hadron collision experiments.

However, when 2-jet events are selected, the fluctuations are found to be anisotropic. The degree of anisotropy depends on the resolution scale ($y_{\rm cut}$) used to identify the 2-jet events.

Having observed the isotropy of dynamical fluctuations in the randomized thrust frame, the intermittency indices are obtained by fitting Equation (10) to the 3-D factorial moments. Both JETSET and, to a lesser extent, HERWIG give reasonable descriptions of both the 3- and 1-dimensional F_q.

Acknowledgments

We are grateful for the participation of G. Chen and L.S. Liu in this study, which was made possible by a Scientific Exchange project (01CDP017) between China (MOST) and The Netherlands (KNAW).

References

[1] See for example Yu. Dokshitzer, V. A. Khoze, A. H. Mueller and S. I. Troyan, *Basics of Perturbative QCD* (Editions Frontières, Giv-sur-Yvette, 1991); G. Altarelli, *The Development of Perturbative QCD* (World Scientific, Singapore, 1994).

[2] B. Mandelbrot, *The Fractal Geometry of Nature*, (W. H. Freeman, New York 1983); B. Mandelbrot, in *Dynamics of Fractal Surfaces*, eds. E. Family and T. Vicsek, (World Scientific, Singapore, 1991).

[3] G. Veneziano, in *Proc. Third Workshop on Current Problems in High Energy Particle Theory*, Florence 1979, eds. R. Casalbnoni *et al.* (Johns Hopkins Univ., Baltimore, 1979), p. 45; K. Konishi, A. Ukawa and G. Veneziano, Phys. Lett. **78B** (1978) 243; Nucl. Phys. **B 157** (1979) 45; A. Giovannini, in *Proc. Xth Int. Symp. on Multiparticle Dynamics*, Goa 1979, eds. S. N. Ganguli, P. K. Malhotra and A. Subramanian, (Tata Inst.) p. 364.

[4] A. Białas and R. Peschanski, Nucl. Phys. **B 273** (1986) 703.

[5] A. Białas and R. Peschanski, Nucl. Phys. **B 308** (1988) 857.

[6] E. A. De Wolf, I. M. Dremin, W. Kittel, Phys. Rep. **270** (1996) 1.

[7] Liu Feng, Liu Fuming and Liu Lianshou, Phys. Rev. **D 59** (1999) 114020.

[8] DELPHI Collab., P. Abreu *et al.*, Nucl. Phys. **B 386** (1992) 471.

[9] T. Sjöstrand, Comp. Phys. Comm. **82** (1994) 74.

[10] OPAL Collab., G. Abbiendi *et al.*, Eur. Phys. J. **C 11** (1999) 239.

[11] NA22 Collab., N. M. Agababyan *et al.*, Phys. Lett. **B 382** (1996) 305.

[12] NA22 Collab., N. M. Agababyan *et al.*, Phys. Lett. **B 431** (1998) 451.

[13] S. Wang, Z. Wang and C. Wu, Phys. Lett. **B 410** (1997) 323.

[14] L3 Collab., B. Adeva *et al.*, Nucl. Instr. Meth. **A 289** (1990) 35;
J.A. Bakken *et al.*, Nucl. Instr. Meth. **A 275** (1989) 81;
O. Adriani *et al.*, Nucl. Instr. Meth. **A 302** (1991) 53;
B. Adeva *et al.*, Nucl. Instr. Meth. **A 323** (1992) 109;
K. Deiters *et al.*, Nucl. Instr. Meth. **A 323** (1992) 162;
M. Acciarri *et al.*, Nucl. Instr. Meth. **A 351** (1994) 300.

[15] JACEE Collab., T. H. Burnett *et al.*, Phys. Rev. Lett. **50** (1983) 2062.

[16] NA22 Collab., M. Adamus *et al.*, Phys. Lett. **B 185** (1987) 200.

[17] Wu Yuanfang and Liu Lianshou, Phys. Rev. Lett. **70** (1993) 3197.

[18] W. Ochs, Phys. Lett. **B 247** (1990) 101.

[19] Wu Yuanfang and Liu Lianshou, Science in China **A 38** (1995) 435.

[20] S. Brandt, Ch. Peyrou, R. Sosnowski and A. Wroblewski, Phys. Lett. **12** (1964) 57.

[21] MARK J Collab., D. P. Barber *et al.*, Phys. Rev. Lett. **43** (1997) 830.

[22] W. Ochs, Z. Phys. **C 50** (1991) 339.

[23] A. Białas and M. Gazdzicki, Phys. Lett. **B 252** (1990) 483.

[24] Liu Lianshou, Zhang Yang and Deng Yue, Z. Phys. **C 73** (1997) 535.

[25] Yu. L. Dokshitzer, J. Phys. **G 17** (1991) 1537.

[26] S. Bethke, Z. Kunszt, D.E. Soper and W.J. Stirling, Nucl. Phys. **B 370** (1992) 310.

[27] D. J. Mangeol, Ph.D. thesis, Univ. of Nijmegen, 2002.

[28] Y. Hu, Ph.D. thesis, Univ. of Nijmegen, 2002.

[29] L. Lönnblad and T. Sjöstrand, Phys. Lett. **B351** (1995) 293.

[30] The L3 detector simulation is based on GEANT, see R. Brun *et al.*, CERN report CERN DD/EE/84-1 (Revised), 1987, and uses GHEISHA to simulate hadronic interactions, see H. Fesefeldt, RWTH Aachen report PITHA 85/02, 1985.

[31] Sw. Banerjee, S. Banerjee, L3 Note 1978 (1996);
J. Casaus, L3 Note 1946 (1996);
S. Banerjee, D. Duchesneau, S. Sarkar, L3 Note 1818 (1995).

[32] Yu. L. Dokshitzer, G. D. Leder, S. Moretti and B. R. Webber, JHEP **8** (1997) 1.

[33] Liu Lianshou, Chen Gang and Fu Jinghua, Phys. Rev. **D 63** (2001) 054002.